IOP Publishing Nanotechnology
Nanotechnology 27 (2016) 335201 (6pp) doi:10.1088/0957-4484/27/33/335201

Spin diffusion and non-local spin-valve effect in an exfoliated multilayer graphene with a Co electrode

Lijun Li[1], Inyeal Lee[1], Dongsuk Lim[1], Servin Rathi[1], Moonshik Kang[1,2], Tetsuya Uemura[3] and Gil-Ho Kim[1]

[1] School of Electronic and Electrical Engineering and Sungkyunkwan University Advanced Institute of Nanotechnology, Sungkyunkwan University, Suwon 16419, Korea
[2] Manufacturing Engineering Team, Memory Division, Samsung Electronics Co., Hwasung 18448, Korea
[3] Division of Electronics for Informatics, Graduate School of Information Science and Technology, Hokkaido University, Sapporo 060-0814, Japan

E-mail: uemura@ist.hokudai.ac.jp and ghkim@skku.edu

Received 21 January 2016, revised 2 May 2016
Accepted for publication 12 May 2016
Published 4 July 2016

Abstract

We fabricated a non-local spin valve with a thin layer of graphite with Co transparent electrodes. The spin-valve effect and spin precession were observed at room temperature. The magnitude of the mangetoresistance increases when temperature decreases. The spin-relaxation time, τ_s, obtained from the fitting of the Hanle curves increases with decreasing temperature with a weak dependence $\sim T^{-0.065}$ while the spin-diffusion constant D decreases. At room temperature, τ_s exceeds 100 ps and the spin-diffusion length, λ_s, is $\sim 2\ \mu$m. The temperature dependence of λ_s is not monotonic, and it has the largest value at room temperature. Our results show that multilayer graphene is a suitable material for spintronic devices.

Keywords: spin diffusion, multilayer graphene, spintronics

(Some figures may appear in colour only in the online journal)

Nanoelectronic devices made by mono- and few-layer graphene operating on the control of the electron spin have attracted great interest in recent years [1]. In a spintronic device, spin transport and injection play important roles in the characteristics of the operation. Natural carbon material, because of its low atomic mass and the natural abundance of isotope ^{12}C (98.9%), is an ideal material for spin manipulation. Spin injection and spin transport in graphene had been observed in non-local spin valves [2, 3]. Long spin-diffusion lengths were reported in boron nitride covered or encapsulated graphene layers in non-local spin-valve geometry [4–6] and in local spin valves with a large injection barrier [7]. When spin current is injected from a ferromagnetic metal into a highly resistive transport channel, the injected spins can be backscattered into the ferromagnetic leads. This is the issue of conductivity mismatch that often takes place in spintronic devices [8–10]. A graphene multilayer, which can be acquired more easily than a mono- or bilayer, has its advantage in spintronic applications. Compared with mono- or bilayer graphene, the multilayer has a higher conductivity, which can provide a preferable condition by reducing the resistance mismatch between the ferromagnetic electrodes and the channel. Spin injection and detection were observed in local and non-local spin valves in multilayer graphene [11–14]. Concerning τ_s in multilayer graphene, there had been early experiments of spin resonance [15] suggesting that in graphite τ_s is ~20 ns at room temperature. Spin-precession measurements had also been applied in multilayer graphene [16, 17]. In these experiments, an enhancement of τ_s with increasing number of layers was observed [16], and the temperature dependence of τ_s in a small temperature range of 150–230 K in a trilayer sample were shown [17]. In this work, we fabricated a graphene multilayer device with Co electrodes. Spin precession and spin-valve effect were measured in the temperature range of 2.2–295 K. The temperature dependence of τ_s and λ_s was obtained from the fitting of the spin-precession Hanle curves.

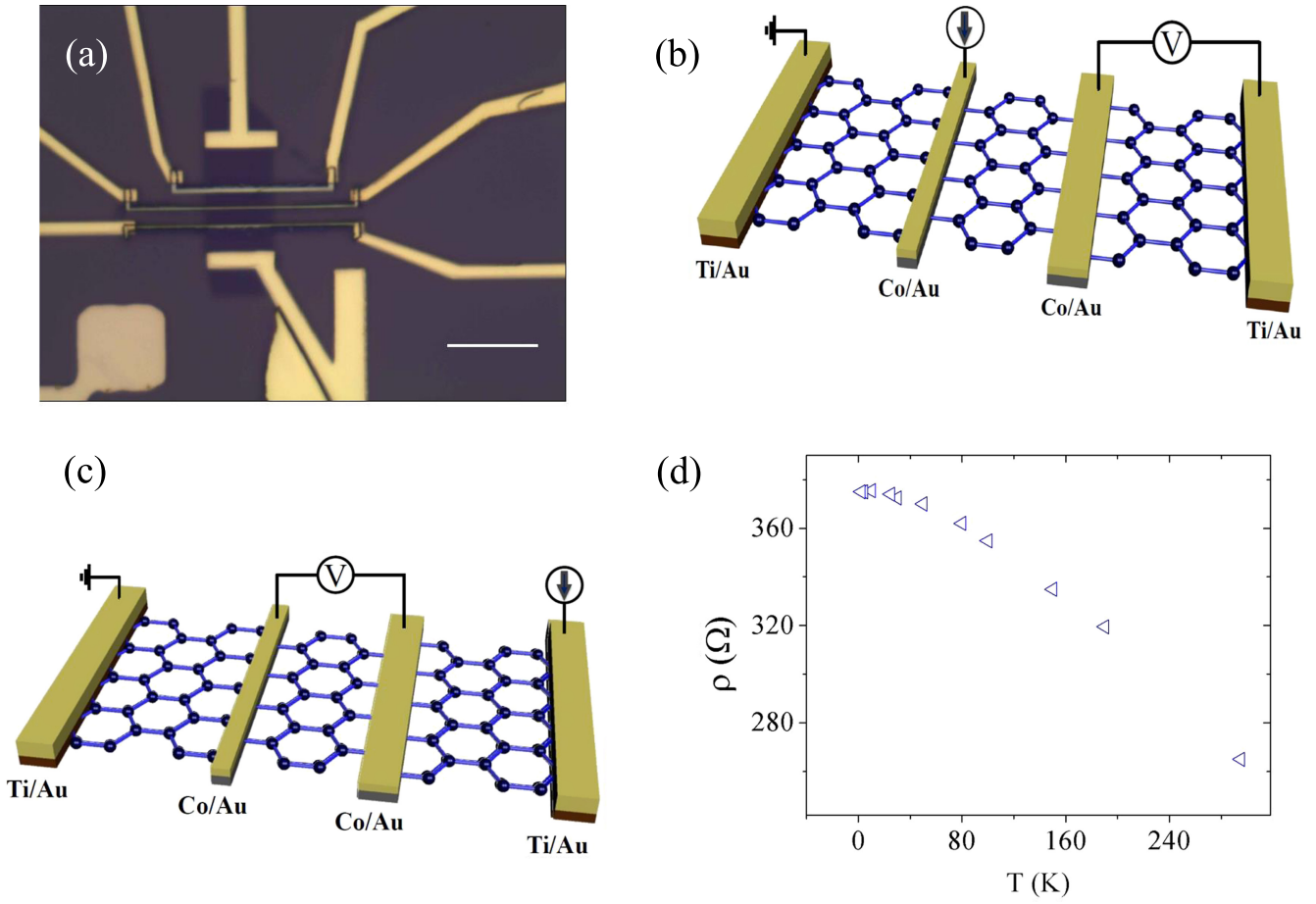

Figure 1. (a) Optical image of the device. The three electrodes in the middle are Co electrodes. From the lower to higher positions the widths of the Co electrodes are 100, 200, 400 nm, respectively. The widths of the Ti/Au electrodes are 2 μm. In the spin precession and four-terminal resistivity measurement, the Co electrodes of 200 and 400 nm are used. The gap between these two Co electrodes is 1.7 μm, the gap between the 400 nm Co and Ti/Au electrode is 4.6 μm and between the 200 nm Co and the other Ti/Au electrode it is 4.8 μm. Scale bar: 10 μm. (b) Schematic showing the non-local electrical measurement for spin-valve and spin-precession experiments. (c) Four-terminal resistivity measurement diagram. (d) Temperature dependence of the layer resistivity measured by methods shown in (c).

The graphene multilayer was exfoliated from highly oriented pyrolytic graphite (HOPG) and deposited on SiO_2 substrate. From our experience with optical contrast, we estimate that the layer consists of 5–10 monolayers (thickness is about 2 nm). The layer was etched by O_2 plasma into a rectangular shape with dimensions of 7×20 μm^2. Electrode patterns were made with e-beam lithography and e-beam evaporation of metals Co/Au (50/3 nm). The thin layer of Au on top of Co is aimed at mitigating Co oxidation. There are three Co electrodes with widths of 100, 200, and 400 nm, respectively. On the two ends of the layer, non-ferromagnetic electrodes Ti/Au (10/100 nm) were deposited with another e-beam lithography process. The electrodes are connected with bonding pads. An optical image of the sample was shown in figure 1(a). In the non-local measurement (figure 1(b)) the Co electrodes used are the ones with widths of 200 and 400 nm.

Current and voltage characteristics between the contacts are linear. An estimation of the contact resistance (interface resistance R_I) shows that both Ti/Au and Co electrodes have an R_I of about 100 Ω. The ratio of R_I and spin resistance R_s of the transport channel is a criterion for conductance mismatch [10], where R_s is given by $\rho\lambda_s/W$, with W the channel width. In this study, R_I/R_s is estimated to be 1.3. Concerning spin injection and detection in these circumstances, while there is no tunneling barrier between the Co electrodes and the graphene layer, the impedance mismatch is not a severe problem. Measurements were performed in a vacuum cryostat ($\sim 10^{-3}$ Torr) and in a helium flowing cryostat with lock-in amplifiers. The current used in the measurements is 70 μA. The magnetoresistance does not depend on the ac current applied. Figure 2 shows the results from the vacuum measurement at temperatures $T = 295$ and 35 K. The spin-valve signal, which was measured in magnetic fields parallel to the electrodes, is larger at lower T, and it increases from 0.028 Ω at 295 K to 0.036 Ω at 35 K. Figures 2(c) and (d) show the spin-precession curves measured in a magnetic field perpendicular to the sample surface with the two Co electrodes magnetized in parallel and antiparallel configurations. Using the analytical expression described in [18], τ_s and λ_s were extracted from the fitting of the spin-precession measurement. When the temperature is lowered, an increase of τ_s but a decrease of λ_s were observed. These fitted results are presented in table 1.

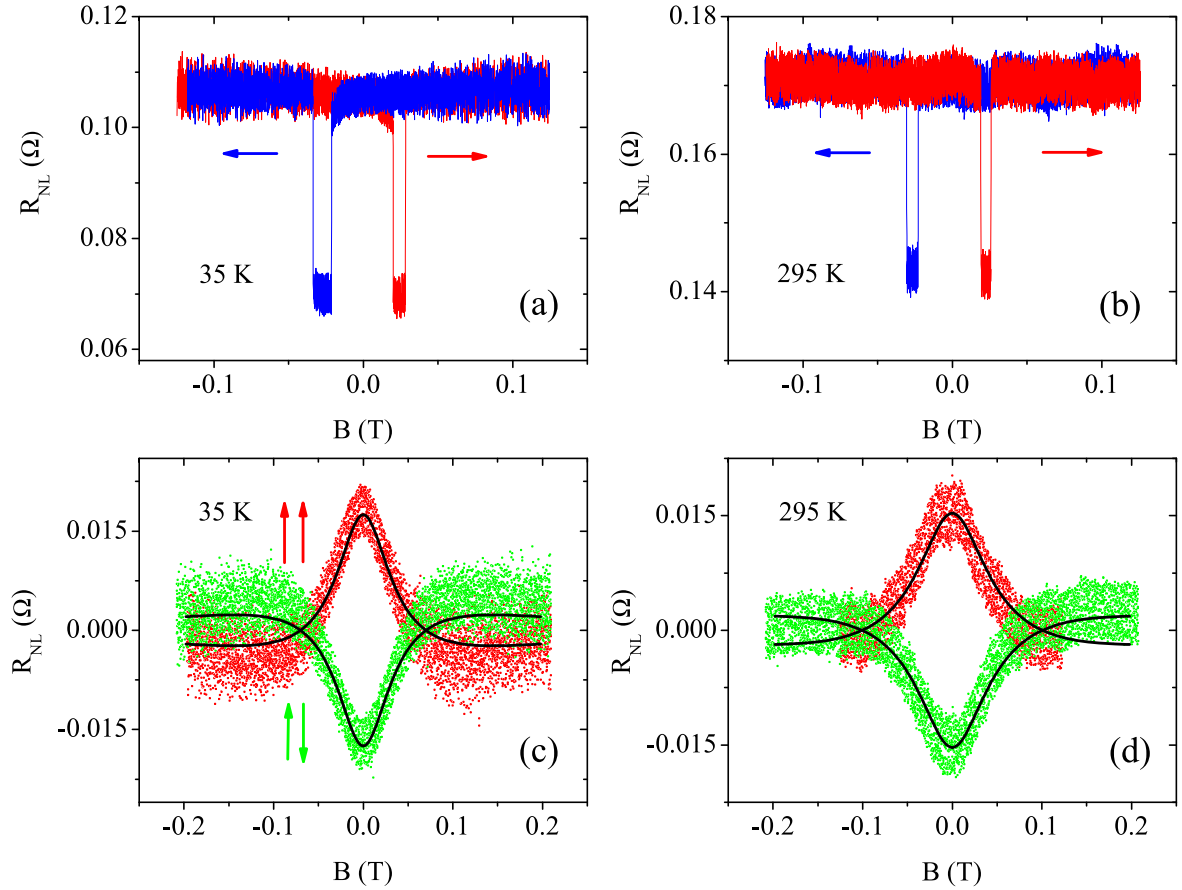

Figure 2. Experimental results measured in a vacuum cryostat. (a), (b) Spin-valve signal measured at 35 and 295 K with magnetic field parallel to the electrodes. Arrows show the magnetic field sweeping direction. (c), (d) Spin-precession Hanle curves measured at magnetic field perpendicular to the sample surface with the two Co electrodes in parallel and antiparallel configurations. Symbols are the experimental results. Solid black lines are the fit from theoretical expression described in [18].

Table 1. Comparison of the fitting results and the calculated spin-diffusion length in the two measurements.

	T (K)	τ_s (ns)	D (m^2 s^{-1})	λ_s (μm)
Vacuum	295 K	0.14	0.025	1.87
Vacuum	35 K	0.18	0.016	1.70
He flow	295 K	0.105	0.038	1.99
He flow	30 K	0.125	0.023	1.69

Measurements in a helium flow cryostat were performed two weeks later. After the vacuum measurements, the sample was coated with PMMA to lesson the device degradation from contamination by air. Before the device was mounted into the helium cryostat, it had been annealed at 60 °C for 30 min in flowing Ar gas (1000 sccm). We expect this annealing process would remove the remaining solvent of PMMA, as well as O_2, H_2O and other air molecules trapped in the PMMA. After annealing, the device was magnetized with the two Co electrodes in parallel configuration and mounted into the helium cryostat. Spin-precession curves were measured from 2.2–295 K. The temperature-dependent zero field resistivity, ρ, was also measured and presented in figure 1(d). With decreasing temperature, ρ increases monotonically from its room T value of 265 Ω to the saturation value of 375 Ω. This saturation takes place at temperatures lower than 25 K. According to previous reports on temperature-dependent resistivity [19, 20], $\rho \sim C/(T^{1-n})$, with n larger than unity, and C denoting a collection of constants. We have checked the data by plotting ρ and T in double logarithm scale, but we found that it does not follow this prediction. We are interested in doing detailed measurement of the temperature-dependent resistivity in the future.

In the fitting of the Hanle results, we used polarization $P = 0.18$. This value was obtained from the fit of the lowest temperature data. When we fitted the higher temperatures, we found that using the same P and varying τ_s and D we can match the experimental curves well. Thus, we set P fixed for all the measured temperatures. For the Co electrode, previous experiments show that the temperature dependence of P is negligible [22]. We used gyromagnetic ratio $g = 2$ in graphite [21]. τ_s and D are set as free fitting parameters. λ_s is then calculated by $\lambda_s = \sqrt{D\tau_s}$. The results at room temperature and at about 30 K have some difference between the vacuum and the He flow measurements, but the trend of change with temperature are the same, see table 1. It is likely that the graphene layer has some change in its electrical property with time and with the coating of PMMA. We have experienced a similar effect in the electrical property of a MoS_2 bilayer

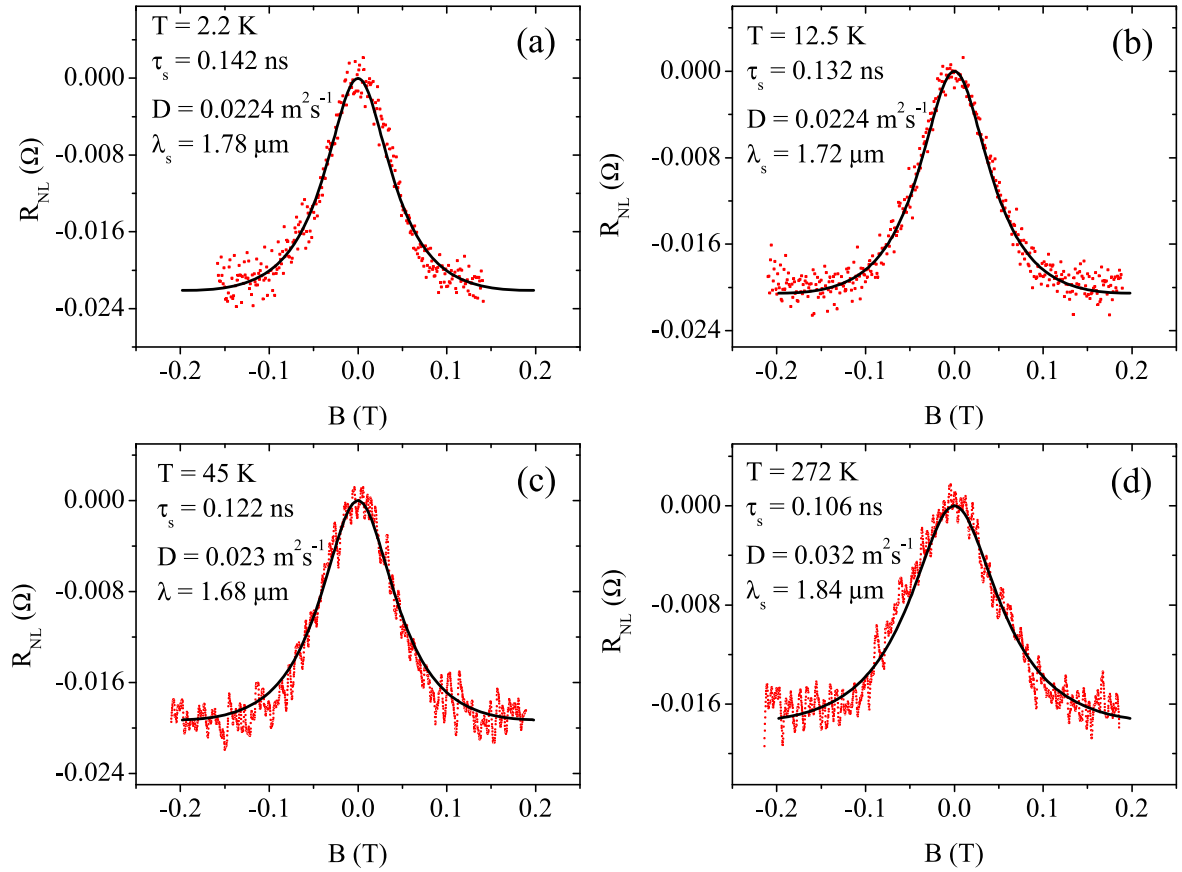

Figure 3. Spin-precession Hanle curves measured in the He flow cryostat at several selected temperatures of $T = 2.2$ K, 12.5 K, 45 K, 272 K. Symbols are experimental results. Black lines are the fit by expression from [18]. The fitted values of τ_s, D and λ_s are shown in the graph.

device [23]. However, it is clear that the spin-transport property does not show significant degradation during a period of two weeks. It should be noted that the analytical expression from [18] works well in the case of tunnel electrodes. Previous works have shown that, for low resistance electrodes, in the absence of considering spin absorption in the injector and detector the Hanle fit leads to deviated values of highly suppressed τ_s and slightly enlarged D [10, 24, 25], depending on the degree of impedance mismatch. In our measurements, $R_I/R_s \approx 1.3$, and $L/\lambda_s \approx 1$ (here L is the distance between the two Co electrodes used in measurement), from figure 3 in [10] we found that the real τ_s is twice the fit value and D should be 10% smaller. Thus, λ_s would be 2.7 μm, i.e. the analysis with expression from [18] gives an underestimated value of λ_s by 25%. In this study, we present the results analyzed without considering the absorption effect. Whether these deviations brought by the analysis would affect the temperature dependence of λ_s significantly or not, we leave for further investigations.

In figures 4(a) and (b) the temperature dependence of τ_s and D were presented. As the temperature decreases τ_s increases but D decreases, similar to the results observed with bilayer graphene [3], but the opposite to that of an epitaxial graphene monolayer on SiC [26]. In our experiments, D changes from 0.038–0.022 m^2 s^{-1} in the temperature range from 295–2.2 K. If we use the 2D density of states and taking valley degeneracy as two [27], from the Einstein relation, the charge-diffusion constant is estimated to be 0.0443 m^2 s^{-1} at 2.2 K and 0.0627 m^2 s^{-1} at 295 K, which are about twice that of the fitted value of the spin-diffusion constant. The charge-diffusion constant is directly proportional to momentum relaxation time τ_p. In exfoliated monolayer graphene, the two values are found to be close [26], but in epitaxial monolayer on SiC, the charge-diffusion constant is several tens times larger [28]. The temperature dependence of λ_s was plotted in figure 4(c). It is interesting to note that λ_s has the largest value at room temperature. This comes from the fact that as the temperature is varied, D changes in the same trend as τ_p, and τ_p is inversely proportional to the layer resistivity. At room temperature, D has its largest value, thus it is possible that λ_s takes a large value. The temperature dependence of τ_s and D in [3] for bilayer graphene also reveals that λ_s is larger at higher temperatures.

In semiconductor materials, there are three spin-relaxation mechanisms: Dyakonov–Perel (DP) spin relaxation caused by spin scattering in a crystal that lacks structure inversion symmetry; Elliott–Yafet (EY) mechanism caused by spin-flip momentum scattering from phonons and impurities with spin–orbit interaction; Bir–Aronov–Pikus (BAP) mechanism caused by spin-flip electron–hole exchange interaction [29]. Theoretical prediction shows that BAP mechanism hardly dominates the spin relaxation in 2D materials [31]. The opposite trend of the temperature

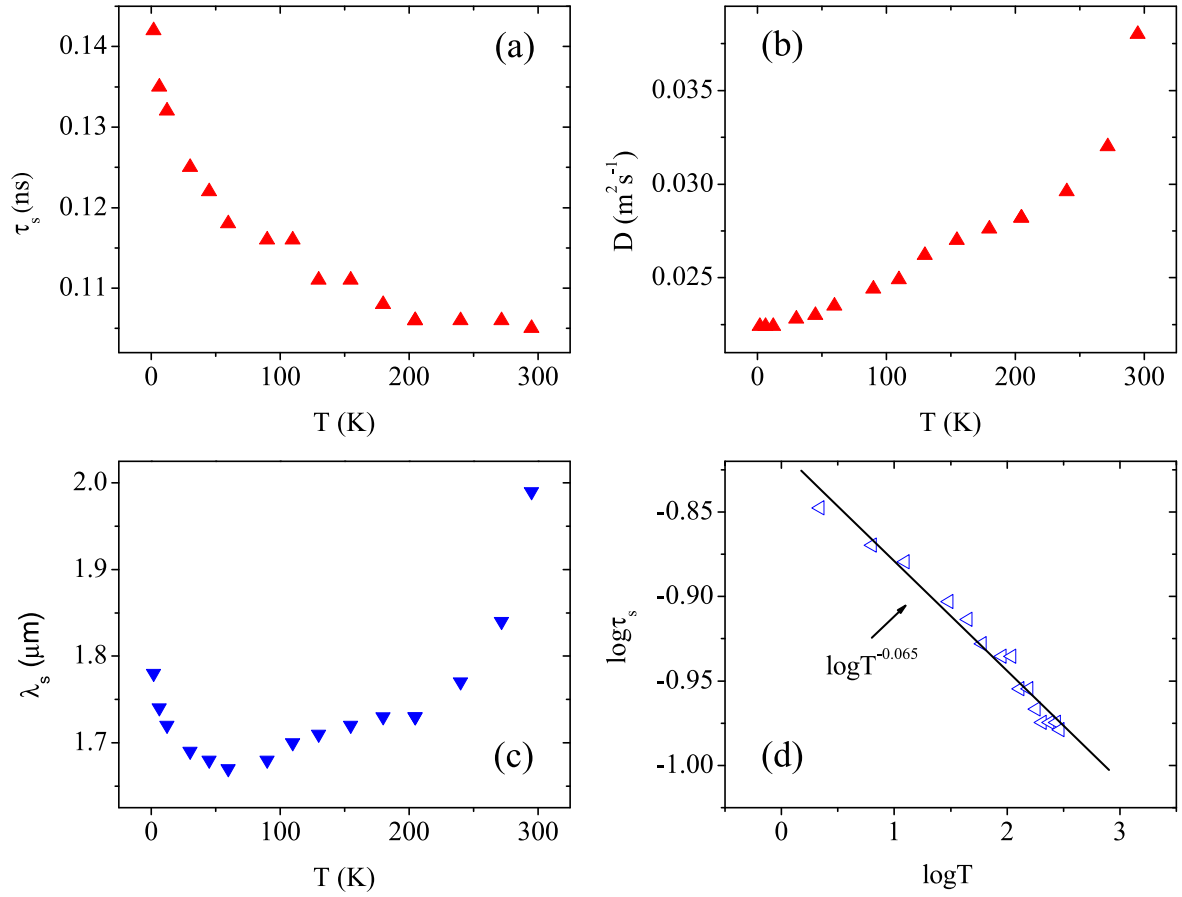

Figure 4. Results obtained in the He flow cryostat. (a) Spin-relaxation time, (b) Diffusion constant, and (c) Spin-diffusion length as a function of temperature T. (d) Plot of log τ_s as a function of log T. Black line is the linear fit of the data. The slope gives -0.065.

dependence of τ_s and D hints at the likely contribution from the DP mechanism. For DP spin scattering, τ_s is inversely proportional to τ_p, i.e. $\tau_s \sim 1/\tau_p \sim \rho$. In our results, at temperatures lower than 200 K and higher than 45 K, τ_s roughly shows a linear dependence on ρ. When τ_s and T were plotted in double logarithm scale, a roughly linear relation was seen (figure 4(d)), and the slope gives $\tau_s \sim T^{-0.065}$. DP mechanism predicts much stronger temperature dependence in bulk material, but in 2D quantum wells the temperature dependence strongly depends on the well width, and in narrow wells the temperature dependence disappears [29, 30]. Previous study [16] on multilayer graphene reported that when charge-carrier density was varied, there is relation $\lambda_s \sim D$, suggesting an EY mechanism. EY mechanism predicts that in graphite $\tau_s \sim T^{-4.5}$, and, in the case without the spin–orbit coupling term, the temperature dependence is linear [32]. Comparing our experimental observation and the theoretical descriptions we infer that in our multilayer graphene, the DP mechanism is the likely cause of spin relaxation.

In summary, we fabricated a multilayer graphene non-local spin valve with Co electrodes. Spin-valve effect and spin precession were observed with this device at room temperature. With decreasing temperature, the spin-relaxation time obtained from the fitting of the Hanle curves increases and follows a $T^{-0.065}$ dependence. The spin-diffusion constant, also a fitted value, decreases with decreasing temperature. We compared our results with spin-relaxation mechanisms in 2D systems. The spin-relaxation length does not depend on temperature monotonically. It takes the largest value at room temperature. Our results show that multilayer graphene can be employed as a suitable material for spintronic devices.

Acknowledgments

This research was supported by the Basic Science Research Program through the National Research Foundation of Korea (NRF) funded by the Ministry of Education, Science and Technology (2013R1A2A2A01069023).

References

[1] Han W, Roland Kawakami K, Gmitra M and Fabian J 2014 *Nat. Nanotechnol.* **9** 794
[2] Tombros N, Jozsa C, Popinciuc M, Jonkman H T and van Wees B J 2007 *Nature* **448** 571
[3] Han W and Kawakami R K 2011 *Phys. Rev. Lett.* **107** 047207
[4] Drögeler M, Volmer F, Wolter M, Terrés B, Watanabe K, Taniguchi T, Güntherodt G, Stampfer C and Beschoten B 2014 *Nano. Lett.* **14** 6050

[5] Zomer P J, Guimaraes M H D, Tombros N and van Wees B J 2012 *Phys. Rev.* B **86** 161416
[6] Guimaraes M H D, Zomer P J, Ingla-Aynés J, Brant J C, Tombros N and van Wees B J 2014 *Phys. Rev. Lett.* **113** 086602
[7] Dlubak B *et al* 2012 *Nat. Phys.* **8** 557
[8] Schmidt G, Ferrand D, Molenkamp L W, Filip A T and van Wees B J 2000 *Phys. Rev.* B **8** R4790
[9] Fert A and Jaffres H 2001 *Phys. Rev.* B **64** 184420
[10] Maassen T, Ver-Marun I J, Guimaraes M H D and van Wees B J 2012 *Phys. Rev.* B **86** 235408
[11] Nishioka M and Goldmana A M 2007 *Appl. Phys. Lett.* **90** 252505
[12] Ohishi M, Shiraishi M, Nouchi R, Nozaki T, Shinjo T and Suzuki Y 2007 *Jpn. J. Appl. Phys.* **46** L605
[13] Wang W H, Pi K, Li Y, Chiang Y F, Wei P, Shi J and Kawakami R K 2008 *Phys. Rev.* B **77** 020402
[14] Goto H, Kanda A, Sato T, Tanaka S, Ootuka Y, Odaka S, Miyazaki H, Tsukagoshi K and Aoyagi Y 2008 *Appl. Phys. Lett.* **92** 212110
[15] Wagoner C 1960 *Phys. Rev.* **118** 647
[16] Maassen T, Dejene F K, Guimaraes M H D, Jozsa C and van Wees B J 2011 *Phys. Rev.* B **83** 115410
[17] Abel J, Matsubayashi A, Garramone J J and LaBella V P 2012 *J. Vac. Sci. Technol.* B **30** 03D115
[18] Sasaki T, Oikawa T, Suzuki T, Shiraishi M, Suzuki Y and Noguchi K 2010 *IEEE Trans. Magn.* **46** 1436
[19] Wallace P R 1947 *Phys. Rev.* **71** 622
[20] Tyler W W and Wilson A C Jr. 1953 *Phys. Rev.* **89** 870
[21] Stankowski J, Waplak S and Bednarski W 2000 *Solid State Commun.* **115** 489
[22] Villamor E, Isasa M, Hueso L E and Casanova F 2013 *Phys. Rev.* B **88** 18441
[23] Li L, Lee I, Lim D, Kang M, Kim G-H, Aoki N, Ochiai Y, Watanabe K and Taniguchi T 2015 *Nanotechology* **26** 295702
[24] Idzuchi H, Takahashi S, Maekawa S and Otani Y 2014 *Phys. Rev.* B **89** 081308
[25] Han W, McCreary K M, Li Y, Wong J J I, Swartz A G and Kawakama R K 2010 *Phys. Rev. Lett.* **105** 167202
[26] Maassen T, van den Berg J J, IJbema N, Fromm F, Seyller T, Yakimova R and van Wees B J 2012 *Nano Lett.* **12** 1498
[27] Koshino M and McCann E 2010 *Phys. Rev.* B **81** 115315
[28] Józsa C, Maassen T, Popinciuc M, Zomer P J, Veligura A, Jonkman H T and van Wees B J 2009 *Phys. Rev.* B **80** 241403
[29] Wu M W, Jiang J H and Weng M Q 2010 *Phys. Rep.* **493** 61–236
[30] Malinowski A, Britton R S, Grevatt T, Harley R T, Ritchie D A and Simmons M Y 2000-I *Phys. Rev.* B **62** 13034
[31] Zhou J and Wu M W 2008 *Phys. Rev.* B **77** 075318
[32] Restrepo O D and Windl W 2012 *Phys. Rev. Lett.* **109** 166604